Accepted Manuscript

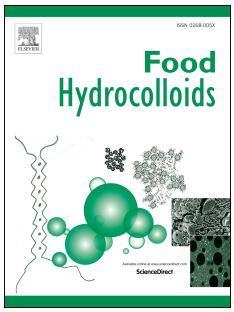

Lamellar structure change of waxy corn starch during gelatinization by time-resolved synchrotron SAXS

Qirong Kuang, Jinchuan Xu, Yongri Liang, Fengwei Xie, Feng Tian, Sumei Zhou, Xingxun Liu

PII: S0268-005X(16)30312-5

DOI: 10.1016/j.foodhyd.2016.07.024

Reference: FOOHYD 3517

To appear in: *Food Hydrocolloids*

Received Date: 12 May 2016

Revised Date: 21 July 2016

Accepted Date: 23 July 2016

Please cite this article as: Kuang, Q., Xu, J., Liang, Y., Xie, F., Tian, F., Zhou, S., Liu, X., Lamellar structure change of waxy corn starch during gelatinization by time-resolved synchrotron SAXS, *Food Hydrocolloids* (2016), doi: 10.1016/j.foodhyd.2016.07.024.

This is a PDF file of an unedited manuscript that has been accepted for publication. As a service to our customers we are providing this early version of the manuscript. The manuscript will undergo copyediting, typesetting, and review of the resulting proof before it is published in its final form. Please note that during the production process errors may be discovered which could affect the content, and all legal disclaimers that apply to the journal pertain.

View metadata, citation and similar papers at core.ac.uk

brought to you by CORE

provided by University of Queensland eSpace

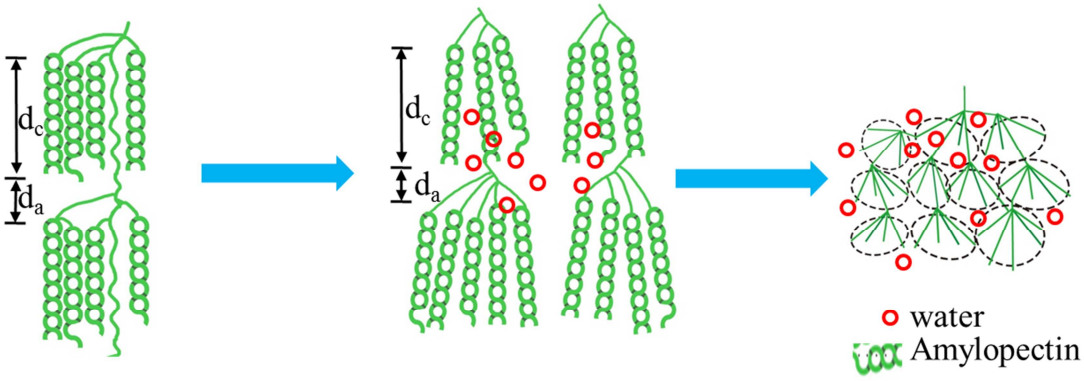

ACCEPTED MANUSCRIPT

ACCEPTED MANUSCRIPT

Lamellar Structure Change of Waxy Corn Starch during Gelatinization by Time-resolved Synchrotron SAXS

Qirong Kuang[a#], Jinchuan Xu[a#], Yongri Liang[b], Fengwei Xie[c], Feng Tian[d], Sumei Zhou[a], Xingxun Liu[a*]

[a] Institute of Food Science and Technology (IFST), Chinese Academy of Agricultural Sciences (CAAS), Beijing, 100193, China

[b] College of Materials and Engineering, Beijing Institute of Petrochemical Technology, Beijing, 102617, China

[c] School of Chemical Engineering, The University of Queensland, Brisbane, Qld 4072, Australia

[d] Shanghai Synchrotron Radiation Facility, Shanghai Institute of Applied Physics, Chinese Academy of Sciences, Shanghai, 201204, China

Corresponding authors:

***** Institute of Food Science and Technology, CAAS, Beijing, China. E-mail: ytboy652@163.com

# These authors contributed equally to this work.

ACCEPTED MANUSCRIPT

Abstract: *In situ* experiment of synchrotron small- and wide-angle X-ray scattering (SAXS/WAXS) was used to study the lamellar structure change of starch during gelatinization. Waxy corn starch was used as a model material to exclude the effect of amylose. The thicknesses of crystalline (d_c), amorphous (d_a) regions of the lamella and the long period distance (d_{ac}) were obtained based on a 1D linear correlation function. The SAXS and WAXS results reveal the multi-stage of gelatinization. Firstly, a preferable increase in the thickness of crystalline lamellae occurs because of the water penetration into the crystalline region. Then, the thickness of amorphous lamellae has a significant increase while that of crystalline lamellae decreases. Next, the thickness of amorphous lamellae starts to decrease probably due to the out-phasing of starch molecules from the lamellae. Finally, the thickness of amorphous lamellae decreases rapidly, with the formation of fractal gel on a larger scale (than that of the lamellae), which gradually decreases as the temperature further increases and is related to the concentration of starch molecular chains. This work system reveals the gelatinization mechanism of waxy corn starch and would be useful in starch amorphous materials processing.

Keywords: waxy starch, lamellar structure, gelatinization, SAXS, synchrotron

ACCEPTED MANUSCRIPT

1. Introduction

Starch is the main component of food and provides an essential energy for humans. Recently, starch has attracted much attention as a renewable polymer resource for eco-friendly uses due to its advantages of biodegradability and low costs (Yu, Dean, & Li, 2006). Starch granules are always heated in water before used, and this results in an order-disorder phase transition, termed "gelatinization". Gelatinization is one of the most significant processing methods in industry and food application of starch, which determines the proper conversion of starch in the processing of food and emerging biodegradable starch-based materials (Liu, et al., 2011).

The structure of native starch granules is a unit entirety and organized in different length scales, *i.e.*, whole granule (μm), growth rings (~0.1 μm), lamellar structure (8-11 nm) and molecular scale (~0.1nm) (Pérez & Bertoft, 2010; Tran, et al., 2011). It is widely recognised that the native starch granule is composed of alternating amorphous and semi-crystalline growth rings. The semi-crystalline growth ring consists of the repeats of alternating amorphous and crystalline lamellae. The amorphous lamellae are related to branch points of the amylopectin side chains, and the crystalline lamellae are formed by the short-chain fractions of amylopectin arranged as double helices and packed in small crystallites, respectively (Witt, Doutch, Gilbert, & Gilbert, 2012). Also, linear amylose molecules and probably less ordered amylopectin are present in an amorphous state within each native granule (Fan, et al., 2013; Pérez, et al., 2010)

In our previous papers (Chen, Yu, Kealy, Chen, & Li, 2007; Chen, et al., 2011), the changes of granule and growth rings of starch during gelatinization have been studied by light microscopy and confocal light scanning microscopy (CLSM). However, there had been no non-destructive and efficient methods to observe the lamellar structure of starch until the use of SAXS. SAXS measures the variations in electron density distributions of amorphous and crystalline lamellae in granule starch (Blazek & Gilbert, 2011). Although the lab SAXS is widely used in starch lamellar

structure characterization (Zhang, Chen, Zhao, & Li, 2013), the lab SAXS is still rarely used for *in-situ* experiments due to its lower light brightness.

Compared with lab-bench SAXS instruments, synchrotron SAXS may offer much higher spectral brilliance, small source size and high beam flux (Koch, 2006). Therefore, synchrotron SAXS is very effective to study the *in-situ* (real time) lamellar structure change during gelatinization. Vermeylen et al. (Vermeylen, et al., 2006a, 2006b) have studied the gelatinization behavior of rice starch and potato starch with bound or limited water by *in-situ* SAXS experiments. It was found that the water content plays a major role in gelatinization and the change of lamellar and crystalline structures during gelatinization. Waigh et al. (Waigh, Gidley, Komanshek, & Donald, 2000) also studied the starch structure change during gelatinization by *in-situ* SAXS and found two different processes for the A-type and B-type starches. However, the SAXS analysis in their study did not investigate the changes in the amorphous and crystalline layers. Yang et al. (Yang, et al., 2016) have used synchrotron SAXS coupled with diamond anvil cell (DAC) to study the effect of high hydrostatic pressure on starch gelatinization and used the correlation function to reveal the change in thickness of the crystalline and amorphous layers during this process.

In this study, synchrotron SAXS and WAXS were used to *in-situ* study the lamellar structure of waxy corn starches during gelatinization. Waxy starches were selected as a model material since there is nearly no amylose starch in its lamellar structure and waxy starch shows a clear peak corresponding to the lamellar phase. The correlation function was used to analyze the *in-situ* synchrotron SAXS results of waxy starch in excess water. Those studies would help to probe the changes in waxy starch amorphous and crystalline layers during gelatinization.

2. Material and Method

2.1 Sample and sample prepared

Waxy corn starch with the amylose/amylopectin ratio of 0/100 was obtained from Lihua Starch Industry Co., Ltd. (Qinhuangdao, China). The amylose content was

determined by the method of concanavalin A while the moisture content (MC) (about 10%) of each sample was determined using a moisture analyzer (MA35, Sartorius Stedim Biotech GmbH, Germany). Distilled water was added to the starch to obtain a starch: water ratio of 1:3 (w/v) in a glass vial and equilibrated 24 h for SAXS/WAXS tests.

2.2 Differential scanning calorimetry

The gelatinization behavior of starch was determined by a differential scanning calorimeter (200 F3, Netzsch, Germany) equipped with a thermal analysis data station. Exactly 3 mg of starch were weighed into an aluminum sample pan. Distilled water was added to the starch in the DSC pans with a pipette to obtain a starch: water ratio of 1:3 (w/v) in the DSC pans. When water was added, care was taken to ensure that the starch granules were completely immersed in the water by gentle shaking. The pans were sealed, and the sealed pans were allowed to stand overnight at room temperature before DSC analysis. An empty pan was used as a reference. The pans were heated from 20 to 120 °C at a scanning rate of 10 °C/min. The analysis was undertaken in triplicate. The software of Netzsch Proteus Thermal Analysis Version 6.1.0 was used to analyze the DSC traces.

2.3 Small and wide Anger X-ray scattering (SAXS/WAXS)

Synchrotron time-resolved small and wide-angle X-ray scattering (SAXS/WAXS) measurements were carried out at BL16B1 beamline at Shanghai Synchrotron Radiation Facility (SSRF), China. We loaded the suspension (0.70 mL) into 2-mm-thick sample cells, of which the front and back windows were both covered with Kapton tape. Two-dimensional (2D) Mar165 were used to collect the 2D SAXS and WAXS patterns. The wavelength of the incident X-ray was 1.24 Å for both SAXS and WAXS, and the sample to detector distance (SDD) was 1940 mm for SAXS and 115 mm for WAXS measurements. A beef tendon specimen and Cerium oxide (CeO_2) were used as standard materials for the calibration of the scattering vector of SAXS and WAXS, respectively. The air and water scattering were subtracted from the

original SAXS and WAXS data. A Linkman (STC200) hot stage was used to control sample temperatures, which was calibrated by a temperature calibrator (Fluker 724) with a K type thermocouple (Omega) before use. The temperature rose from 35 to 85 °C, at a speed of 2 °C/min, with a holding time of 1 min. Data were collected at each degree rise and were measured for 60 seconds. 2D SAXS and WAXS patterns were recorded by a Mar165 charge-coupled device (CCD) detector. By measuring sample adsorption using ionization chambers in front and back of the sample cell, we performed data correction, calibrated the SAXS data from the background scattering, and normalized the data on the primary beam intensity. Background subtraction follows the equation: $I_s(\theta)=I_t(\theta)-\frac{I_t}{I_b}\frac{T_t}{T_b}I_b(\theta)$. $I_t(\theta)$, $I_b(\theta)$ and $I_s(\theta)$ represent the distribution of scattering intensity of samples held in cells, sample cells and pure samples respectively. I_t and I_b represent the values of samples held in cells and sample cells, read from the ionization chambers in front of sample cell. T_i and T_t represent the transmissivity of samples held in cells and sample cells.

2.4 SAXS analysis

The normalized 1D correlation function $\gamma_1(r)$ is defined as

$$\gamma_1(r) = \int_0^\infty I(q)q^2\cos(qr)dq / Q$$

where $\underline{I}(q)$ is scattering intensity, q is scattering vector defined as $q=4\pi\sin\theta/\lambda q$ (2θ is the scattering angle) and r is the direction along the lamellar stack.

The scattering invariant, Q, is defined as

$$Q = \int_0^\infty I(q)q^2dq$$

Because of the finite q range of experimental SAXS data, extrapolation of the 1D SAXS data to both the low and high q ranges are necessary for the integration of the intensity, I(q). Extrapolation to low q was performed using an intensity profile based on Guinier's law, and the extension of the intensity to large q values can be accomplished using the Porod-Ru land model (Yang, Liang, & Han, 2015; Yang, Liang, Luo, Zhao, & Han, 2012). The parasitic scattering and thermal fluctuation were corrected using a normalized 1D correlation function.

3. Result and Discussion

3.1 Thermal behavior by DSC

DSC is a quick and efficient method to test gelatinization behavior of starch. Corn starch with different amylose content has been studied before using DSC (Chen, et al., 2007). From Fig.1, it can be seen that the waxy starch exhibited a significant gelatinization endotherm at about 71°C, which has been well accepted as the representation of the gelatinization of amylopectin. The onset, peak and end temperature of waxy starch used in this experiment are 60, 71 and 83°C, respectively. According to previous studies (Liu, Yu, Xie, & Chen, 2006; Liu, et al., 2013), DSC with a stainless steel pan could be used to study the phase transition during gelatinization.

3.2 SAXS curves analysis

The SAXS one-dimensional (1D) scattering intensity distributions for waxy starch at different temperatures are shown in Fig. 2A and Fig. 2B. It is clearly seen that there is one typical scattering peak around the q value of 0.6-0.7nm^{-1} in each SAXS curves below the temperature of 70.7°C, indicating a 9-10 nm semi-crystalline structure according to Bragg's law $D=2\pi/q$. No typical scattering peak was observed above 72.9°C. In fact, the scattering peak indicated a long period (also known the lamellar repeat distance, or Bragg spacing) in granule starches (Blazek, et al., 2011). The position of SAXS peak is reciprocally related to the average total thickness of the crystalline and amorphous regions in lamellar arrangements (Waigh, Perry, Riekel, Gidley, & Donald, 1998). Moreover, the intensity depends on the amount of the ordered semi-crystalline structures and/or on the differences in electron density between crystalline and amorphous lamellae on the amorphous background (Yuryev, et al., 2004).

From Fig.2A and Fig.2B, it could be clearly seen that the peak intensity decreased with increasing temperature. This reduction means that the destruction to crystalline lamellae may lead to a reduction in the electron density contrast between crystalline and amorphous lamellae. However, there are several rises in peak intensity,

as the temperature went from 61.8°C to 66.3°C. Meanwhile, the peak becomes broadening with increasing temperature. In fact, the peak width depends on the regularity of the lamellar arrangements within the starch granule (Blazek, et al., 2011; Yang, et al., 2016).

To further analyze the SAXS curves, Lorentz correction was used, and the selected temperature could be found in Fig.3. The peak intensity shows similar trends as in Fig.2. Scattering invariant (Q) is proportional to the electron density difference between the crystalline and amorphous phases, and the volume fractions of the two phases are based on a two-phase model. From Fig.2, it could be seen that Q increased firstly and then decreased. Correspondingly, the contrast of electron density was firstly enhanced, which should be due to the water uptake and swelling in the amorphous parts and/or the leaching of amylose from the amorphous parts. The decrease in peak intensity suggests a gradually decreasing electron density contrast between amorphous and crystalline lamella. However, a slight increase of the peak between 61.8 °C and 66.3 °C is observed, which is a new phenomenon and needs to be studied in the future.

3.3 SAXS analysis with correlation function

The 1D correlation function can provide the structure parameters of lamellar structures of polymers (Chen, et al., 2016; Yang, et al., 2012). Recently, the correlation function is widely used in the analysis of starch aggregation structure and provides basic structure parameters such as the thickness of crystalline (d_c), amorphous (d_a) region of the lamella and long period distance ($d_{ac}= d_a+d_c$) (Chen, et al., 2016; Fan, et al., 2013; Yang, et al., 2016). In this method, the long period distance (d_{ac}) is the value of x at the second maximum of γ_1(x), d_a is representing the solution of linear regression in the auto correlation triangle (LRAT) at y = value of the flat minimum of $\gamma(x)$. Hence, the average thickness of the crystalline lamellae d_c, equals (d_{ac} - d_a) (Goderis, Reynaers, Koch, & Mathot, 1999).

The normalized 1D correlation function can be seen in Fig. 4, where we assigned the larger layer thickness to the amorphous and crystalline thickness. Fig.5

shows the temperature function of d_c, d_a, and d_{ac} and the Bragg lamellar repeat distance, D (D=2π/q). From Fig.5, it could be seen that the long period distance (d_{ac}) from the correlation function have a proper fitting with D from Bragg's law. A significant decrease in D, d_{ac} and d_c, as well as an increase in d_a above 70 °C, could be clearly observed. However, when the temperature is below 70 °C, D and d_{ac} remain almost identical at approx. 8.5 nm. It is noteworthy that d_c rises slightly with the temperature increasing from 50 to 55 °C, before it decreases to around 6.4 nm. A slight increase in d_c could be seen along with the temperature rising from 65 to 70 °C. An opposite trend is observed in d_a, which is as expected since d_{ac} did not change greatly. The side-chain model (Waigh, et al., 2000) could explain the increase in the thickness of crystalline lamellae, implying that the amylopectin branching points could be compressed by the double helices of the amylopectin side chains because of the plasticization of the spacers.

3.4 WAXS analysis

The time-resolved wide-angle X-ray diffractogram is shown in Fig.6. A typical A-type crystalline structure can be observed with peaks near 15°, 17°, 18° and 23°. WAXS is always used to study the longer range scale structure of starch crystallites, which mainly consists of monoclinic and/or hexagonal crystal units (Zhang, et al., 2015). From Fig.6, the peak intensity gradually becomes weaker as the temperature increases, indicating the reduction in crystallinity and increase of amorphous zones. Peaks are almost invisible at 72.7 °C, showing the absence of crystalline structure. This is consistent with results from SAXS and DSC, which results from gelatinization.

3.5 Starch gel structure analysis

The fractal dimension indicates the compactness of a system (Beaucage, 1996) and has been used to describe the self-similar structure of gel structure (Tamon & Ishizaka, 1998). In the low-q region the curves comply with a simple power law equation (Zhu, Li, Chen, & Li, 2012), $I(q) \sim q^{-\alpha}$, where the exponent α gives insight into the surface/mass fractal structure. Moreover, the mass fractal dimension

253 ($0 < \alpha < 3$) is used to indicate the compactness, whereas the surface fractal dimension
254 ($3 < \alpha < 4$) is regarded as an indicator of the degree of smoothness of the scattering
255 objects.

256 After gelatinization, starch becomes a gel. From Fig.7, it could be seen that the
257 exponent α decreased from 2.70 to 1.21 (within the q of 0.1 to 0.2 nm^{-1}, the
258 corresponding size of 31.4 nm to 62.8 nm) with the increasing temperature from 75
259 to 85^{o}C, which means the starch gel is a mass fractal structure. Moreover, α till
260 decreases when the temperature keeps at 85 °C for 1 min. These results suggest that
261 the scattering objects of gelatinized waxy starch were more compact with the
262 increasing temperature. Since the SAXS measurements were performed *in-situ*, the
263 measured change in the starch gel fractal structure could depend on the concentration
264 of amylopectin, and a high concentration may lead to a mass fraction. This
265 phenomenon will be studied by rheology and *in-situ* SAXS in future.

266 **3.6 Gelatinization mechanism from SAXS/WAXS**

267 Generally, the well-accepted conception of "gelatinization" means destroying the
268 crystalline structure in the starch granule (Liao, et al., 2014; Xie, et al., 2006), which
269 is an irreversible multi-stage process including granule swelling, native crystalline
270 melting, loss of birefringence and starch solubilization (Sullivan & Johnson, 1964).
271 SAXS and WAXS would provide the information of lamellar and crystallinity
272 structure change during gelatinization.

273 Starch suspensions with a higher concentration were used in this study as a model
274 system to reveal the gelatinization mechanism. The simply lamellar structure changes
275 during heating for waxy starch could be found in Fig.8. The results of d_a, d_c and d_{ac}
276 from SAXS by a correlation function would further clarify the changes of the starch
277 lamellar structure. (A) First, water is slowly and reversibly taken up in the
278 crystallinity lamellar with the increasing temperature although the water is already
279 equilibrated in starch (Chen, et al., 2007; Liu, et al., 2011). At this stage, the size of
280 amorphous lamellar does not change, but the size of crystallinity lamellar has a slight
281 increase. (B) From 55 to 60 °C (T_o, onset temperature), the size of amorphous
282 lamellar has a modest increase. This phenomenon is also observed in the

gelatinization caused by ultra-high hydrostatic pressure (Yang, et al., 2016). However, the reduction of the size of crystallinity lamellar is unexpected. (C) After the onset temperature, the amorphous lamellar starched to decrease probably due to the out-phasing of starch molecules from them (Zhang, et al., 2015). Meanwhile, the SAXS intensity has a clear increase. (D) From T_p, the decrease of d_c could attribute to the disrupted crystalline layer, and all amylopectin double helices are dissociated to form a gel.

4. Conclusion

Gelatinization is essential for industry and food application of starch. The present study investigated the lamellar structure of starch during gelatinization. *In situ* synchrotron SAXS and WAXS are used in this work. Waxy starches were selected as model materials since there is no amylose starch in its lamellar structure and waxy starch shows a clear peak corresponding to the lamellar phase. The correlation function was used to analyze the in situ synchrotron SAXS results of waxy starch in excess water.

During gelatinization, WAXS intensity decreases gradually with the increasing temperature, and the temperature for the disappearance of the WAXS peak is consistent to that of the DSC and SAXS lamellar peaks. The thickness of crystalline (d_c), amorphous (d_a) regions of the lamellae and the long-period distance (d_{ac}) were obtained from a 1D linear correlation function. The average thicknesses of amorphous layers and crystalline layers show different change trends with the increasing temperature.

Overall, the multiple stages of gelatinization could be concluded: firstly, a preferable increase in the thickness of the crystalline lamellae because of the water penetration into crystalline regions; then, the thickness of amorphous lamellae has a significant increase while that of crystalline lamellae decreases; next, the amorphous lamellae start to decrease probably due to the out-phasing of starch molecules from them; at last, the thickness of amorphous lamellae decreases rapidly with the formation of fractal gel on a larger scale (than that of the lamellae) which gradually

decreases as the temperature increases further and is related to concentration of starch molecular chains. This work reveals the gelatinization mechanism of waxy corn starch and would be useful in starch amorphous materials processing.

Conflict of interest

The authors declare that there is no conflict of interests regarding the publication of this paper.

Acknowledgments

The authors from China would like to acknowledge the research funds from the Natural Science Foundation of China (NSFC) under the Project No. 31301554.

References

Beaucage, G. (1996). Small-Angle Scattering from Polymeric Mass Fractals of Arbitrary Mass-Fractal Dimension. *Journal of Applied Crystallography, 29*(2), 134-146.

Blazek, J., & Gilbert, E. P. (2011). Application of small-angle X-ray and neutron scattering techniques to the characterisation of starch structure: A review. *Carbohydrate Polymers, 85*(2), 281-293.

Chen, P., Wang, K., Kuang, Q., Zhou, S., Wang, D., & Liu, X. (2016). Understanding how the aggregation structure of starch affects its gastrointestinal digestion rate and extent. *International Journal of Biological Macromolecules, 87*, 28-33.

Chen, P., Yu, L., Kealy, T., Chen, L., & Li, L. (2007). Phase transition of starch granules observed by microscope under shearless and shear conditions. *Carbohydrate Polymers, 68*(3), 495-501.

Chen, P., Yu, L., Simon, G. P., Liu, X. X., Dean, K., & Chen, L. (2011). Internal structures and phase-transitions of starch granules during gelatinization. *Carbohydrate Polymers, 83*(4), 1975-1983.

Fan, D., Wang, L., Ma, S., Ma, W., Liu, X., Huang, J., Zhao, J., Zhang, H., & Chen, W. (2013). Structural variation of rice starch in response to temperature during microwave heating before gelatinisation. *Carbohydrate Polymers, 92*(2), 1249-1255.

Goderis, B., Reynaers, H., Koch, M. H. J., & Mathot, V. B. F. (1999). Use of SAXS

and linear correlation functions for the determination of the crystallinity and morphology of semi-crystalline polymers. Application to linear polyethylene. *Journal of Polymer Science Part B: Polymer Physics, 37*(14), 1715-1738.

Koch, M. H. J. (2006). X-ray scattering of non-crystalline biological systems using synchrotron radiation. *Chemical Society Reviews, 35*(2), 123-133.

Liao, L., Liu, H., Liu, X., Lin, Yu, L., & Chen，, P. (2014). Microstructures and phase transitions of starch. *Acta Polym Sinica*.

Liu, H., Yu, L., Xie, F., & Chen, L. (2006). Gelatinization of cornstarch with different amylose/amylopectin content. *Carbohydr Polym, 65*(3), 357-363.

Liu, P., Xie, F., Li, M., Liu, X., Yu, L., Halley, P. J., & Chen, L. (2011). Phase transitions of maize starches with different amylose contents in glycerol-water systems. *Carbohydrate Polymers*.

Liu, X., Wang, Y., Yu, L., Tong, Z., Chen, L., Liu, H., & Li, X. (2013). Thermal degradation and stability of starch under different processing conditions. *Starch - Stärke, 65*(1 - 2), 48-60.

Pérez, S., & Bertoft, E. (2010). The molecular structures of starch components and their contribution to the architecture of starch granules: A comprehensive review. *Starch - Stärke, 62*, 389-420.

Sullivan, J. W., & Johnson, J. A. (1964). Measurement of starch gelatinization by enzyme susceptibility. *Cereal Chemistry, 41*, 73-79.

Tamon, H., & Ishizaka, H. (1998). SAXS Study on Gelation Process in Preparation of Resorcinol–Formaldehyde Aerogel. *Journal of Colloid and Interface Science, 206*(2), 577-582.

Tran, T. T. B., Shelat, K. J., Tang, D., Li, E., Gilbert, R. G., & Hasjim, J. (2011). Milling of Rice Grains. The Degradation on Three Structural Levels of Starch in Rice Flour Can Be Independently Controlled during Grinding. *Journal of Agricultural and Food Chemistry, 59*(8), 3964-3973.

Vermeylen, R., Derycke, V., Delcour, J. A., Goderis, B., Reynaers, H., & Koch, M. H. J. (2006a). Gelatinization of Starch in Excess Water: Beyond the Melting of Lamellar Crystallites. A Combined Wide- and Small-Angle X-ray Scattering Study. *Biomacromolecules, 7*(9), 2624-2630.

Vermeylen, R., Derycke, V., Delcour, J. A., Goderis, B., Reynaers, H., & Koch, M. H. J. (2006b). Structural Transformations during Gelatinization of Starches in Limited Water: Combined Wide- and Small-Angle X-ray Scattering Study. *Biomacromolecules, 7*(4), 1231-1238.

Waigh, T. A., Gidley, M. J., Komanshek, B. U., & Donald, A. M. (2000). The phase transformations in starch during gelatinisation: a liquid crystalline approach. *Carbohydrate Research, 328*(2), 165-176.

Waigh, T. A., Perry, P., Riekel, C., Gidley, M. J., & Donald, A. M. (1998). Chiral Side-Chain Liquid-Crystalline Polymeric Properties of Starch. *Macromolecules, 31*(22), 7980-7984.

Witt, T., Doutch, J., Gilbert, E. P., & Gilbert, R. G. (2012). Relations between Molecular, Crystalline, and Lamellar Structures of Amylopectin. *Biomacromolecules, 13*(12), 4273-4282.

Xie, F. W., Liu, H. S., Chen, P., Xue, T., Chen, L., Yu, L., & Corrigan, P. (2006). Starch Gelatinization under Shearless and Shear Conditions. *International Journal of Food Engineering, 2*(5).

Yang, J., Liang, Y., & Han, C. C. (2015). Effect of crystallization temperature on the interactive crystallization behavior of poly(l-lactide)-block-poly(ethylene glycol) copolymer. *Polymer, 79*, 56-64.

Yang, J., Liang, Y., Luo, J., Zhao, C., & Han, C. C. (2012). Multilength Scale Studies of the Confined Crystallization in Poly(l-lactide)-block-Poly(ethylene glycol) Copolymer. *Macromolecules, 45*(10), 4254-4261.

Yang, Z., Gu, Q., Lam, E., Tian, F., Chaieb, S., & Hemar, Y. (2016). In situ study starch gelatinization under ultra-high hydrostatic pressure using synchrotron SAXS. *Food Hydrocolloids, 56*, 58-61.

Yu, L., Dean, K., & Li, L. (2006). Polymer blends and composites from renewable resources. *Progress in Polymer Science, 31*(6), 576-602.

Yuryev, V. P., Krivandin, A. V., Kiseleva, V. I., Wasserman, L. A., Genkina, N. K., Fornal, J., Blaszczak, W., & Schiraldi, A. (2004). Structural parameters of amylopectin clusters and semi-crystalline growth rings in wheat starches with different amylose content. *Carbohydrate Research, 339*(16), 2683-2691.

Zhang, B., Chen, L., Xie, F., Li, X., Truss, R. W., Halley, P. J., Shamshina, J. L., Rogers, R. D., & McNally, T. (2015). Understanding the structural disorganization of starch in water-ionic liquid solutions. *Physical Chemistry Chemical Physics, 17*(21), 13860-13871.

Zhang, B., Chen, L., Zhao, Y., & Li, X. (2013). Structure and enzymatic resistivity of debranched high temperature–pressure treated high-amylose corn starch. *Journal of Cereal Science, 57*(3), 348-355.

Zhu, J., Li, L., Chen, L., & Li, X. (2012). Study on supramolecular structural changes of ultrasonic treated potato starch granules. *Food Hydrocolloids, 29*(1), 116-122.

ACCEPTED MANUSCRIPT

Figures

ACCEPTED MANUSCRIPT

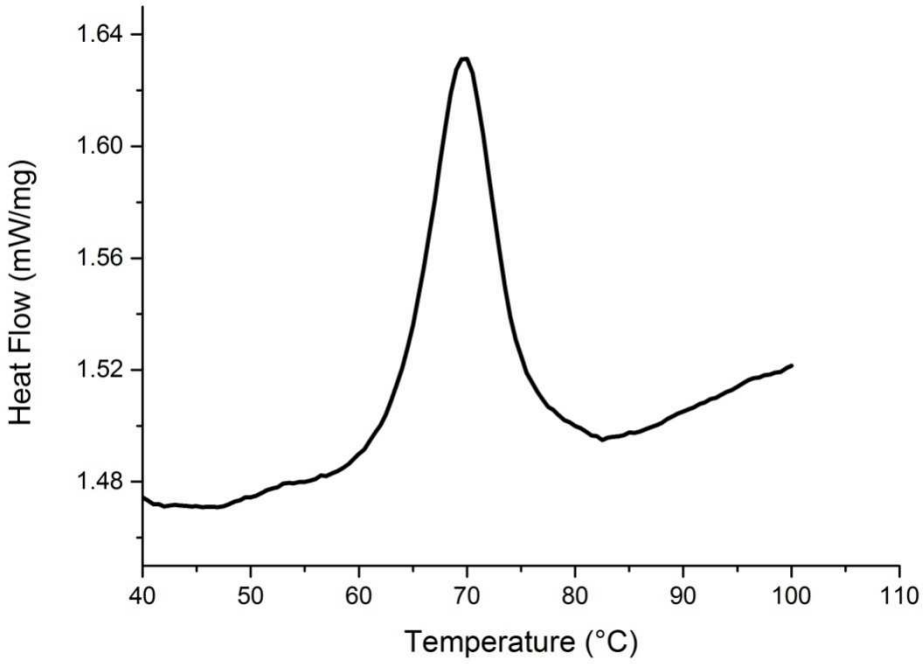

Fig.1 DSC thermograms of native waxy cornstarch in abundant water.

ACCEPTED MANUSCRIPT

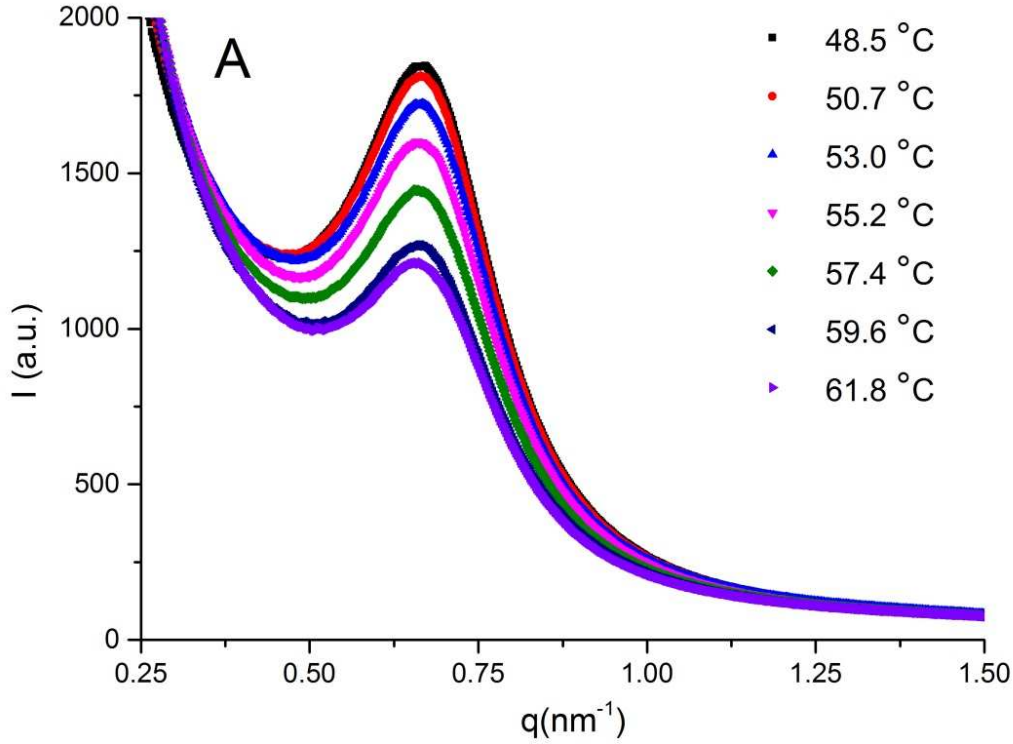

11

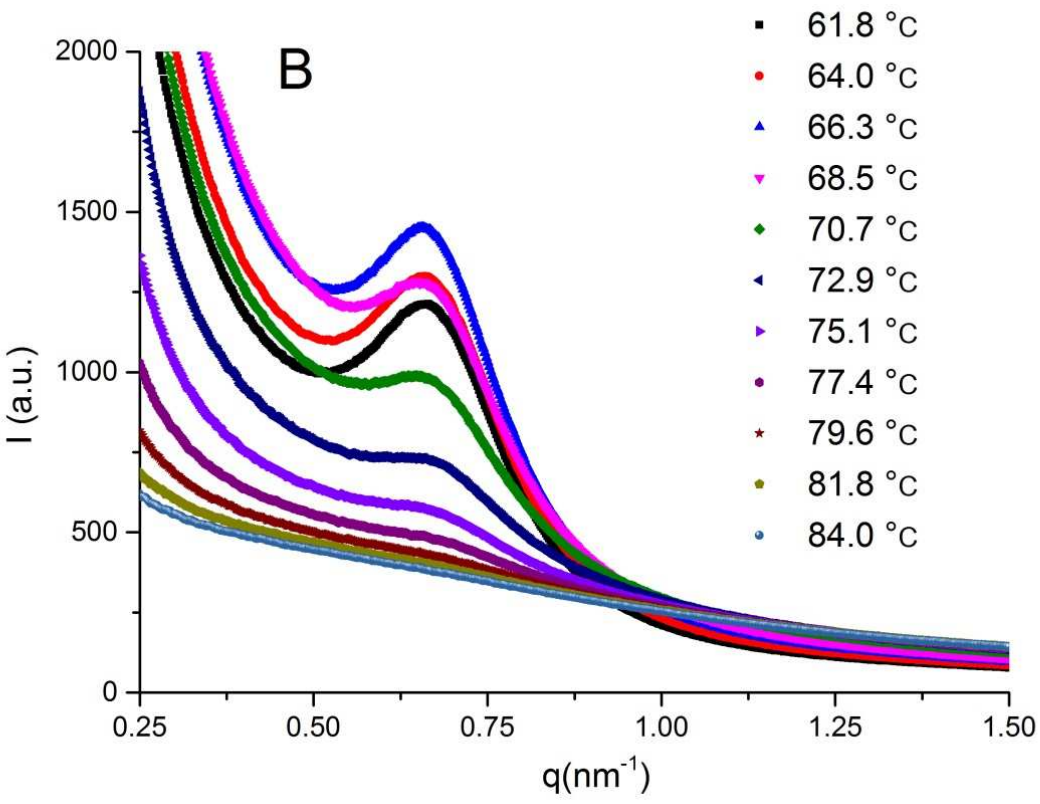

12

13 Fig.2 *In-situ* synchrotron SAXS patterns of waxy corn starch at different temperatures

14 (A) 40-61.8°C; (B) 61.8-84°C.

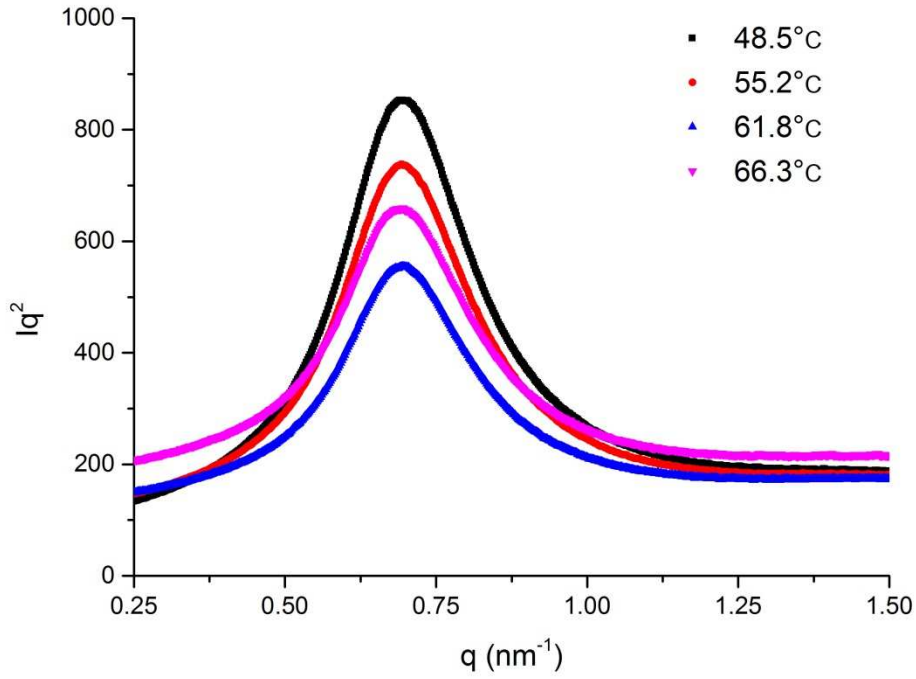

Fig.3 Lorentz-corrected 1D SAXS profiles of waxy corn starch under selected temperature

ACCEPTED MANUSCRIPT

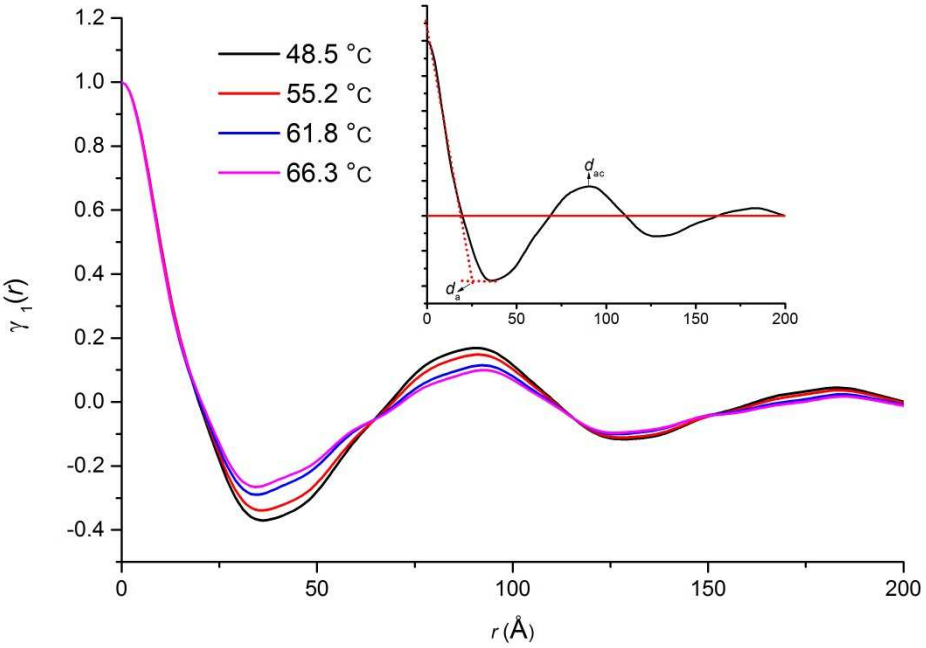

Fig.4 Normalized 1D correlation function of waxy corn starch

ACCEPTED MANUSCRIPT

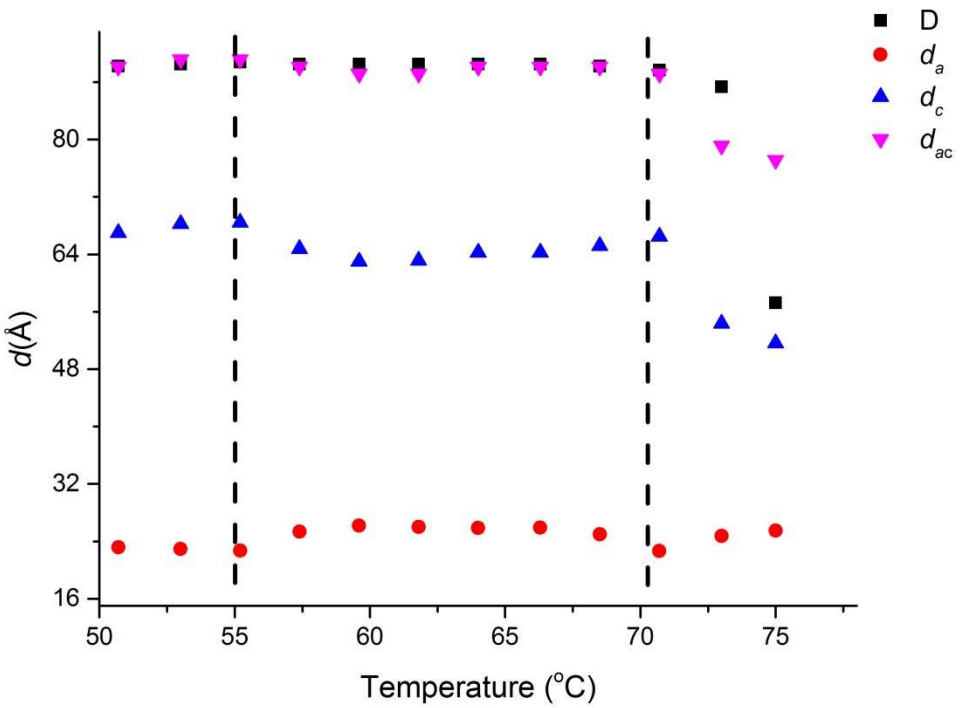

Fig.5 Changes in Bragg lamellar repeat distance (D), long period (d_{ac}), thickness of amorphous layer (d_a) and thickness of crystalline layer (d_c) as a function of temperature for waxy corn

ACCEPTED MANUSCRIPT

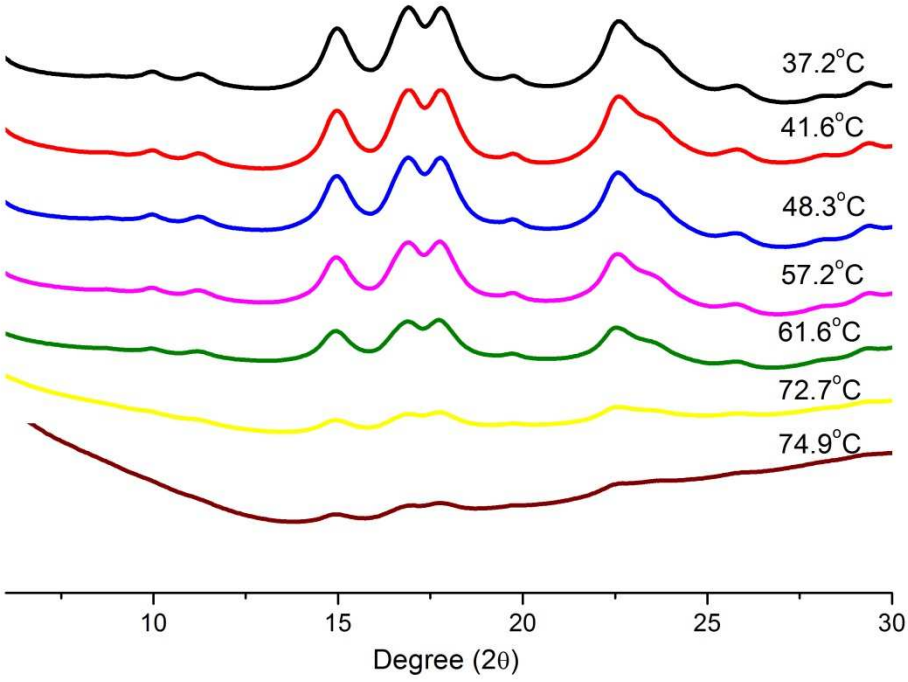

Fig.6 *In-situ* synchrotron WAXS patterns of waxy corn starch at different temperatures

ACCEPTED MANUSCRIPT

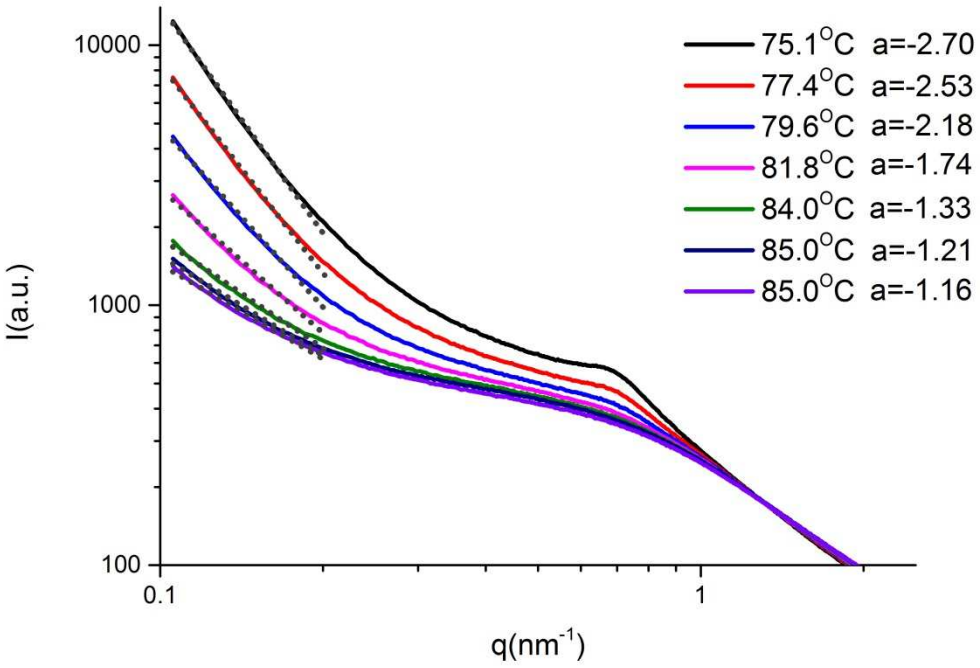

Fig.7 SAXS patterns (log-log) of waxy corn starches. The black scatting dot lines show the relationship $I \sim q^{\alpha}$ at selected temperature (the last 85 °C means this temperature was kept for 1 min.)

ACCEPTED MANUSCRIPT

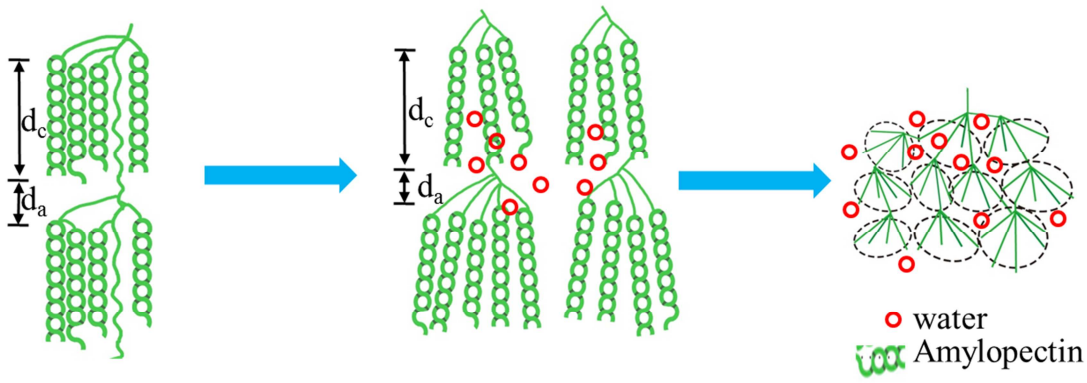

79

80

81 Fig. 8 Schematic representation for waxy starch lamellar structure changes during
82 heating.

83

84

ACCEPTED MANUSCRIPT

ACCEPTED MANUSCRIPT

Highlights

1. In situ SAXS/WAXS is used to study the lamellar structure change during gelatinization for waxy corn starch.

2. The multi-stage of gelatinization of starch is observed

3. The lamellar structure change for starch is a function of temperature.

4. Starch gel shows a mass fractal structure.

ACCEPTED MANUSCRIPT